



24th COBEM - 2017



24th ABCM International Congress of Mechanical Engineering
December 3-8, 2017, Curitiba, PR, Brazil

COBEM-2017-0801

ADAPTATION OF A NONLINEAR LIFTING LINE BASED METHOD INTO A VORTEX LATTICE CODE FOR STALL AND POST STALL CALCULATION

Alexandre Martins Araújo

Ricardo Luiz Utsch de Freitas Pinto

Department of Mechanical Engineering – Federal University of Minas Gerais

Center for Aeronautical Studies - CEA

Av. Antônio Carlos, 6627, 31270-901, Belo Horizonte – MG, Brazil

utsch@demec.ufmg.br

Danilo César Rodrigues Azevedo

danilo.azevedo@ufpi.edu.br

Abstract. *This paper presents the implementation of a method, presented in the literature, adapted for partially stalled surfaces, based on the classic lifting line formulation, into a nonlinear vortex lattice code utilized in the university, with its iterative method also presented in the literature, but not able to get reasonable results after stall. After the implementation, the results were compared with experimental data presented in other reports to guarantee the reliability of the new method.*

Keywords: *Aerodynamics, Stall, Non-Linear Lifting-Line Theory, Vortex-Lattice*

1. INTRODUCTION

During certain phases of the design process of an aircraft, there is a need for the calculation of the stall characteristics of the aerodynamic surfaces. There are many ways to perform this task, from potential flow solvers, coupled with viscous corrections, to heavy fluid mechanics codes, solving the more general equations of fluid mechanics. Depending on the phase of the aircraft design, it is more desirable a faster method, with sufficiently accurate estimations, than more detailed ones.

One of these faster methods is the vortex-lattice, a potential flow based procedure for calculation of multiple aerodynamic surfaces. When coupled with aerodynamic data of the airfoil, it can lead to sufficiently accurate results. There are some methods in the literature to perform this coupling, but a considerable number of them are not able to get reasonable results when the surface is partially stalled, degrading the estimation of the maximum lift and the analysis of the stall progress of the aerodynamic surfaces.

The vortex-lattice code utilized in many projects in UFMG is called CEA-VLM, originally developed in the work of Vargas (2006). It is based on the Wessinger's method, applying a spanwise distribution of horseshoe vortices. The coupling between the potential flow and the section data is based on the method presented by Mukherjee, *et al.* (2003), where the normal vector of the panel is redirected by an angle in the chordwise direction (δ) to match the resulting forces.

The problem is that, as presented by Araújo (2016), the iteration scheme of this method diverges when the local angle of attack reaches or passes the stall angle, leading to unreasonable results. To overcome that, the nonlinear method presented by Chattot (2004) was implemented in the code, adapting its formulation to the variables of the program. The method is based on the classical lifting line equations, changing the local circulation ($\Delta\Gamma_j$) to guarantee the coupling between local section data and potential flow resulting forces, even when the section is stalled. This new method guaranteed the convergence of the local angle of attack during stall analysis and, comparing with experimental data provided in the literature (Purser and Spearman, 1951), led to better estimations of the maximum lift coefficient and stall angle of the surfaces analyzed.

2. REVIEW

This section presents the analysis methods more important to the work, all available in the literature. They are divided in Classical Theories, where its most important characteristic is the linearity of the results and the assumption of zero viscosity of the flow; and the Nonlinear Methods, which add up some elements to the Classical Theories. In this case, the coupling between the potential flow and the section data, containing information about the viscous part of the flow (friction drag, pressure drag and stall).

2.1 Classical theories

In the so-called ‘‘Classic Aerodynamics’’, all the methods are based on the use of singularity flows that meets the Laplace’s equation, considering an incompressible fluid and irrotational flow (Anderson, 1984). Because of the linearity of the equation, the linear combination of different singularities (that meets some boundary condition) also attends the equation.

All the following methods apply this idea, using vortical flow, or vortex filaments, as the singularity, however, they have different approaches to the creation of a boundary condition, for the obtainment of a single solution for the combination of singularities.

2.1.1 Prandtl’s lifting line

One of the first methods for analysis of lifting surfaces, where the wing is treated as an infinite distribution of spanwise horseshoe vortices, with the bound vortex attached to the ¼ chord line. The method treats each section with a global angle of attack (α) and with an induced angle of attack (α_i), created by the free vortices of all span sections, as shown in Fig.1.

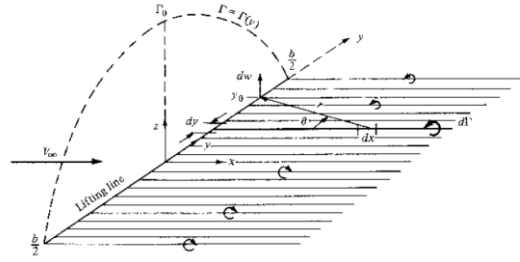


Figure 1. Representation of the distribution of horseshoe vortices (Anderson, 1984)

With the both induced and global angles of attack, one can obtain an effective angle of attack of the section. By relating the lift coefficient with the effective angle of attack, using section airfoil data or, in this case, by assuming it is linear (below the stall region) and by use of the Kutta-Joukowski’s theorem in Eq. (1), it is obtained a closed equation for the intensity distribution of the horseshoe vortices, or, in other words, the circulation distribution, as shown by Eq. (2).

$$\rho_{\infty} V_{\infty} \Gamma(y_0) = \frac{1}{2} \rho_{\infty} V_{\infty}^2 c(y_0) C_L(y_0) \quad (1)$$

$$\alpha = \frac{\Gamma(y_0)}{c(y_0) \pi V_{\infty}} + \alpha_0(y_0) + \frac{1}{4\pi V_{\infty}} \int_{-b/2}^{b/2} \frac{(d\Gamma/dy) dy}{y_0 - y} \quad (2)$$

Where y is the coordinate in the spanwise direction, y_0 is the location of the current section in the analysis, α_0 is the zero-lift angle of attack of the section, c the local chord, ρ_{∞} and V_{∞} the freestream density and velocity, b the span of the lifting surface and Γ the local circulation. Solving Eq. (1) for the given variables, the circulation distribution can be obtained. From that, the forces, such as lift and induced drag, can also be calculated.

From Eq. (1), it is possible to observe the application of the boundary condition in the method, that is, the compatibilization of the local lift force, obtained from the airfoil lift coefficient, and the one calculated from the Kutta-Joukowski’s theorem. This is the core of many nonlinear methods, including the ones applied for vortex-lattice codes. The Prandtl’s method is linear most because of the assumption of a linear airfoil lift coefficient curve (Anderson, 1984).

Moreover, the third term on the right side of Eq. (2) corresponds to the induced velocity generated by the free vortices. In the Prandtl’s method, only their contribution is considered, since the control point is located at the lifting

line ($1/4$ chord line). Because of that, this technique yields sufficiently accurate results for surfaces with low values of sweep angle (Katz and Plotkin, 2001).

2.1.2 Weissinger's method

Known as Extended Lifting Line, in the Weissinger's method, as in the Prandtl's theory, the surfaces are treated as a distribution of horseshoe vortices, with the bound vortex also placed at the $1/4$ chord line. The difference lies in the application of the boundary conditions and the control point. This time, the idea is to obtain a circulation distribution where the total velocity, including the freestream and the ones induced by the vortices, is null in the normal direction of the body at the control point, also known as the non-penetration condition (Katz and Plotkin, 2001). As for the Kutta condition, it approximately complies with the positioning of the control point at the $3/4$ chord line (Katz and Plotkin, 2001). Figure 2 illustrates the panel of a section of the surface.

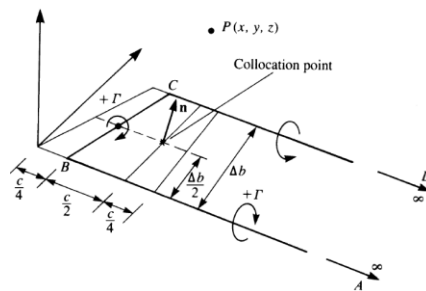


Figure 2. Panel of a surface with the positioning of the control point and the vortex (Katz and Plotkin, 2001)

The calculation of the induced velocity vector at the control point is performed utilizing the Biot-Savart Law, integrated in a finite vortex filament, shown in Fig. 3. For implementation purposes, in the CEA-VLM code, the horseshoe vortices are composed by one small filament located at the $1/4$ chord line of the panel (the bound vortex) and other two filaments in the direction of the free stream that are extremely long. Equation 3 presents the induced velocity vector of a finite filament for a unitary circulation, also known as the influence coefficient.

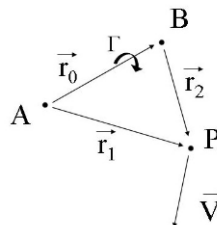


Figure 3. Characteristic vectors of a finite vortex filaments (Vargas, 2006).

$$\vec{a}_{AB,P} = \frac{1}{4\pi} \frac{\vec{r}_1 \times \vec{r}_2}{|\vec{r}_1 \times \vec{r}_2|^2} \left[\vec{r}_0 \cdot \left(\frac{\vec{r}_1}{|\vec{r}_1|} - \frac{\vec{r}_2}{|\vec{r}_2|} \right) \right] \quad (3)$$

Where $\vec{a}_{AB,P}$ is the influence coefficient vector. For every j th panel, all the three coefficients (concerning the bound vortex and the two free vortices) are summed with respect to the control point of the i th panel, building a linear system presented in Eq. (3), applying the non-penetrating boundary condition.

$$\left(\sum_{j=1}^N \vec{a}_{ij} \Gamma_j + \vec{V}_\infty \right) \cdot \vec{n}_i = 0 \quad (3)$$

Where n_i is the unitary vector in the normal direction of the panel. Solving the linear system of Eq. (3) gives the circulation of each panel. By applying the Kutta-Joukowski's theorem on the bound vortex of each panel, the forces (lift and induced drag) are obtained. Since the basis of the method are elementary flows that meets the Laplace's equation, which considers that the fluid is incompressible and inviscid, the method itself cannot get reasonable results next to the surface's stall angle, as in the Prandtl's method. However, since the control point is located at the $3/4$ chord line, the method is able to get better estimations of forces and circulation distribution than the Lifting Line approach in surfaces with higher sweep angles (Katz and Plotkin, 2001).

2.2 Nonlinear methods

All the methods presented herein manipulate the potential solution of the previously cited methods, aiming an increment of the viscous information of the flow presented in the airfoil section data (curves of lift, drag and moment coefficients versus the angle of attack of the airfoil), including friction and pressure drag and stall characteristics.

2.2.1 Decambering

The nonlinear procedure of the code CEA-VLM is based on the work of Mukherjee, *et al.* (2003). It is an iterative method which the main idea is to change the geometrical angle of attack of each section, based on the airfoil section data, changing the non-penetrating boundary condition of the Wessinger's method. The procedures of the iterations are described below.

1. The linear solution from Wessinger's method is obtained for iteration n , utilizing the local "free stream" angle of attack α_{sec} (Section 2.1.2);
2. The effective angle of attack is calculated from Eq. (4);

$$\alpha_{eff} = \frac{C_{Lsec}}{2\pi} - \delta_n \quad (4)$$

Where δ is the decambering angle of each panel (equal to zero in the first iteration) and C_{Lsec} the local lift coefficient, calculated from the Kutta-Joukowski's theorem, using the free stream dynamic pressure and panel area as references;

3. With the effective angle of attack, the viscous lift coefficient (C_{Lvisc}) is obtained from the local airfoil section data. Then, the difference between C_{Lvisc} and C_{Lsec} is computed as the variable ΔC_L ;
4. A new decambering angle is calculated from ΔC_L , using Eq. (5), and the local "free stream" angle of attack is incremented, as shown by Eq. (6);

$$\delta_{n+1} = \delta_n + \frac{\Delta C_L}{2\pi} \quad (5)$$

$$\alpha_{sec} = \alpha + \delta_{n+1} \quad (6)$$

5. With the new value of α_{sec} , a new solution of the linear system of the Wessingers's method is possible, returning to step 1, until the absolute value of ΔC_L is lower than a certain tolerance.

With this procedure, the method can couple the potential flow solution with the local airfoil lift coefficient curve. The problem appears once the iteration reaches an effective angle of attack where the lift curve slope is negative, when the values of C_{Lvisc} and C_{Lsec} start to diverge. When this happens, the effective angle of attack continues to rise, since the value of ΔC_L rises as well, until it reaches the last angle in the section data. At this point, inside the code, for higher angles, all the coefficients are equal. Because of that, the iteration procedure starts to converge again, since it is only necessary the convergence of the parameter C_{Lsec} (and, virtually, the slope is no longer negative). The final consequence is that, when the effective angle of attack is higher than the stall angle, the method converges to the limit angle of the local airfoil curves (Mello, 2014).

2.2.2 Chattot's method

In the formulation of this methodology, presented in the work of Chattot (2004), the surface is treated as a positioning of jx nodes (correspondent to the free vortices) along the span at a distance y from the center; and $jx-l$ integration points (correspondent to the control points of the Prandtl's method), located between the nodes, at a distance η from the center.

From the Kutta-Joukowski's theorem, the local circulation may be written in the form presented in Eq. (7), relating it with the panel lift coefficient, for a unitary speed and semi-span.

$$\Gamma(\eta) = \frac{1}{2} c(\eta) C_L[\alpha_{eff}(\eta)] \quad (6)$$

Where c is the chord of the surface at the integration point. The connection to the airfoil section data is created by the term $C_L[\alpha_{eff}(\eta)]$, that is, the lift coefficient is a function of the effective angle of attack, in other words, the one obtained from the lift curve of the airfoil. Considering the velocity triangle on each integration point, the effective angle of attack may be written as shown by Eq. (7).

$$\alpha_{eff}(\eta) = \alpha - \alpha_0(\eta) + \tan^{-1}[w_{ind}(\eta)] \quad (7)$$

Where w_{ind} is the velocity induced by the free vortices (located at the nodes), that is related to the circulation by the discretization of the Biot-Savart's law, as presented by Eq. (8).

$$w_{ind_j} = -\frac{1}{4\pi} \sum_{k=1}^{jx-1} \frac{\Gamma_{k+1} - \Gamma_k}{\eta_k - y_j}, \quad j = 1, \dots, jx-1 \quad (8)$$

Where the index j represents each integration point. Equations (6) to (8) are the basis of the method, and by the location of the nodes and the integration points, the method is similar to the Lifting Line. Since there is no analytical function relating C_L and α_{eff} , it is necessary an iterative method to find a circulation distribution that attends Eq. (6). This procedure is initiated by the linearization of this same equation, resulting in Eq. (9).

$$\Gamma_j + \Delta\Gamma_j = \frac{1}{2} c_j \left(C_{L_j} + \Delta\alpha_{eff_j} \left. \frac{dC_{L_j}}{d\alpha} \right|_{\alpha=\alpha_{eff_j}} \right) \quad (9)$$

Where $\Delta\Gamma$ is the variation of the circulation in the integration point. The porpoise of the linearization is to relate this parameter to the change of other variables. In Eq. (9), it is related to change of effective angle of attack ($\Delta\alpha_{eff}$). Applying the same logic into Eq. (7) and Eq. (8).

$$\Delta\alpha_{eff_j} = \frac{\Delta w_{ind_j}}{1 + (w_{ind_j})^2} \quad (10)$$

$$\Delta w_{ind_j} = -\frac{1}{4\pi} \left(\frac{1}{y_j - \eta_{j-1}} - \frac{1}{y_j - \eta_j} \right) \Delta\Gamma_j = a_j \Delta\Gamma_j \quad (11)$$

Noting that the linearization is performed by means of a “discrete derivation” in relation to the circulation of the panel itself, so all terms dependent on the circulation of other panels in Eq. (8) become null. The variable a_j in Eq. (11) is similar to the influence coefficient presented in Eq. (3), correspondent to the influence of the panel free vortices on their own integration point. This logic will be used in the implementation of this method into the CEA-VLM code (Section 3).

Placing Eq. (11) into Eq. (10), then into Eq. (9) and isolating the term $\Delta\Gamma$, the variation of circulation due to the airfoil lift coefficient is obtained, or, in other words, the n iteration step, as can be shown by Eq. (12).

$$\Delta\Gamma_j = \omega^+ \frac{\frac{1}{2} c_j C_{L_j} - \Gamma_j^n}{1 - \frac{1}{2} \frac{a_j}{1 + (w_{ind_j})^2} c_j \left. \frac{dC_{L_j}}{d\alpha} \right|_{\alpha=\alpha_{eff_j}}} \quad (11)$$

Where ω^+ is a relaxation factor.

However, after the stall, the sign of the airfoil lift curve slope becomes negative, allowing the denominator of Eq. (11) to become negative (since a_j is always negative), depending on the value of the slope. This fact leads to the divergence of the method (Chattot, 2004). Therefore, to correct this problem, it is introduced an “artificial viscosity” μ in the denominator, with its estimated contribution in the numerator, as shown by Eq. (12).

$$\Delta\Gamma_j = \omega^- \frac{\frac{1}{2} c_j C_{L_j} - \Gamma_j^n + \mu(\Gamma_{j+1}^n - 2\Gamma_j^n + \Gamma_{j-1}^n)}{1 - \frac{1}{2} \frac{a_j}{1 + (w_{ind_j})^2} c_j \left. \frac{dC_{L_j}}{d\alpha} \right|_{\alpha=\alpha_{eff_j}} + 2\mu} \quad (12)$$

The coefficient μ is arbitrary but must have a value high enough to make the denominator positive when the slope is negative. Consequently, the artificial viscosity may be written according to Eq. (13).

$$\mu = \kappa \frac{a_j}{1 + (w_{ind_j})^2} c_j \frac{dC_{L_j}}{d\alpha} \Big|_{\alpha=\alpha_{eff_j}} \quad (13)$$

Where κ is an arbitrary positive coefficient, that must be higher than 0,25. With the formulation presented, the iterative method is completed, following the scheme detailed below.

1. From the geometry of the surface, and the distribution of nodes and integration points, the influence of each free vortex on each integration point is computed and, therefore, the coefficient a_j is obtained;
2. An initial circulation distribution is estimated. This can be performed by means of both Wessinger's and Prandtl's method;
3. The induced speed on each integration point is calculated from Eq. (8), and with that, the effective angle of attack, using Eq. (7);
4. With the airfoils lift curves, the lift coefficient and the slope of the curve are interpolated using the effective angle of attack, on each integration point;
5. Using all the data gathered on each integration point, the variation of circulation $\Delta\Gamma$ is computed by means of Eq. (11) or Eq. (12), depending on the sign of the lift curve slope estimated before;
6. Through the addition of the initial values of circulation with $\Delta\Gamma$, a new distribution is obtained, returning to step 3 until the maximum absolute value of $\Delta\Gamma$ is lower than a certain tolerance.

It must be noted that the formulation of the Chattot's method is closer to the Lifting Line approach than the Wessinger's method. Therefore, many its characteristics, and defects, are present in the method described. However, it has a different approach for stalled panels, and, as it will be shown later, it leads to more reasonable results.

3. FORMULATION CHANGES FOR IMPLEMENTATION

Since the software CEA-VLM makes use of dimensional variables, and the formulation presented in the work of Chattot (2004) assumes a unitary value of velocity and semi-span, it was necessary an adaptation before the actual implementation of the method.

The main change happens in the Kutta-Jukowky's theorem. Considering the values of the panel span and the freestream velocity in the formulation, Eq. (14) is deduced.

$$\Gamma_j = \frac{1}{2} c_j V_j C_{L_j} \quad (14)$$

Where V is the freestream speed. Note that the span of the panel disappears from Eq. (14) since the reference area for the lift coefficient is the span itself times the chord.

Another change in the formulation was applied in the deduction of the effective angle of attack, since, in the original formula, the freestream speed was also considered to be unitary. Therefore, considering the actual velocity in the panel, Eq. (15) is obtained.

$$\alpha_{eff_j} = \tan^{-1} \left(\frac{V_{n_j}}{V_{m_j}} \right) \quad (15)$$

Where V_n and V_m are the local velocities in the normal direction and the chordwise direction, respectively, considering even the velocities induced by the horseshoe vortices.

With these changes, the same procedures are carried on as in the original formulation (Section 2.2.2), resulting in changes on the final equations of the iterative method, all shown in the Eq. (16) to (18).

$$\Delta\Gamma_j = \omega^+ \frac{\frac{1}{2} c_j V_j C_{L_j} - \Gamma_j^n}{1 - \frac{1}{2} c_j V_j \frac{(\vec{a}_{jj} \cdot \vec{n}_j)}{V_{m_j} \left[1 + \left(\frac{V_{n_j}}{V_{m_j}} \right)^2 \right]} \frac{dC_{L_j}}{d\alpha} \Big|_{\alpha=\alpha_{eff_j}}} \quad (16)$$

$$\Delta\Gamma_j = \omega^- \frac{\frac{1}{2}c_j V_j C_{L_j} - \Gamma_j^n + \mu(\Gamma_{j+1}^n - 2\Gamma_j^n + \Gamma_{j-1}^{n+1})}{1 - \frac{1}{2}c_j V_j \frac{(\vec{a}_{jj} \cdot \vec{n}_j)}{V_{m_j} \left[1 + \left(\frac{V_{n_j}}{V_{m_j}} \right)^2 \right]} d\alpha \Big|_{\alpha=\alpha_{eff}} + 2\mu} \quad (17)$$

$$\mu = \kappa c_j V_j \frac{(\vec{a}_{jj} \cdot \vec{n}_j)}{V_{m_j} \left[1 + \left(\frac{V_{n_j}}{V_{m_j}} \right)^2 \right]} d\alpha \Big|_{\alpha=\alpha_{eff}} \quad (18)$$

Where a_{jj} is the influence coefficient vector of the horseshoe vortex on its own panel.

4. RESULTS AND VERIFICATION

The formulation adapted from Chattot's method, presented in Section 3, was implemented into the CEA-VLM code. To verify the procedure, as well the method itself, the results were compared with experimental data presented in the report made by Purser and Spearman (1951), for a determined group of wings. The airfoil lift and drag coefficient curves, for each wing, were obtained from the experimental data given by the report of Sheldahl and Klimas (1981), interpolated for the Reynolds number of each section of the wing, given its geometry and the velocity of the experiment.

Tables 1 to 4 presents the geometrical characteristics and Fig. 4 to 7 the mesh of each wing analyzed.



Figure 4. Mesh of the Wing 1

Table 1. Geometrical data of Wing 1

Span	1,524 m
Root chord	0,254 m
Tip chord	0,254 m
Aspect Ratio	6
Sweep at ¼ chord line	0°
Airfoil	NACA 0012

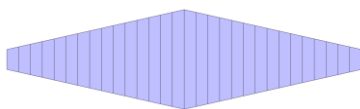


Figure 5. Mesh of the Wing 2

Table 2. Geometrical data of Wing 2

Span	1,524 m
Root chord	0,423 m
Tip chord	0,085 m
Aspect Ratio	6
Sweep at ¼ chord line	6,34°
Airfoil	NACA 23012

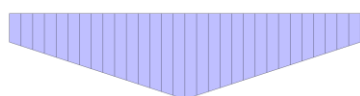


Figure 6. Mesh of the Wing 3

Table 3. Geometrical data of Wing 3

Span	1,524 m
Root chord	0,381 m
Tip chord	0,127 m
Aspect Ratio	6
Sweep at ¼ chord line	14,04°
Airfoil	NACA 23012

Table 4. Geometrical data of Wing 4

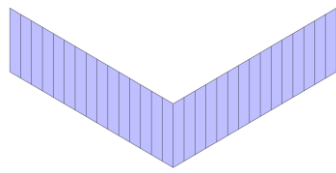


Figure 7. Mesh of the Wing 4

Span	1,524 m
Root chord	11,54 in
Tip chord	11,54 in
Aspect Ratio	5,2
Sweep at ¼ chord line	30°
Airfoil	NACA 0015

Figures 8 to 11 present the results comparison. In then, it is possible to observe the bad behavior of the original code for angles of attack near the stall. Furthermore, the estimative of the maximum lift coefficient from CEA-VLM 2.0 was more accurate for the wings 1 and 3, and for all wings, the drag estimation was better as well.

The results for wing 4 supports the statement that, since the new method implemented is closer to the Lifting Line method than the original one, it carries most of its characteristics and defects. In this analysis, the new formulation lost accuracy for the estimative of the maximum lift coefficient for wings with high sweeps, which is the case of the wing 4.

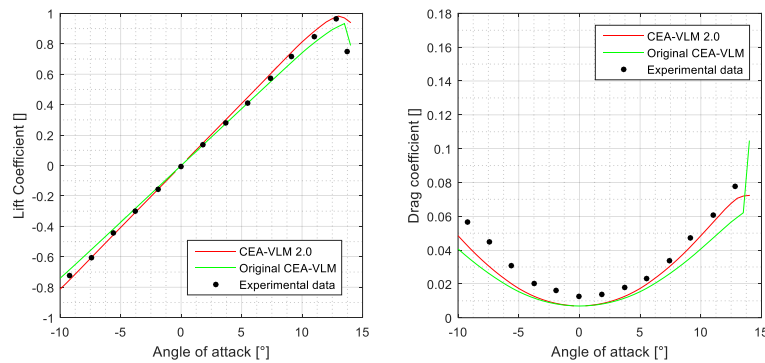


Figure 8. Results comparison for Wing 1

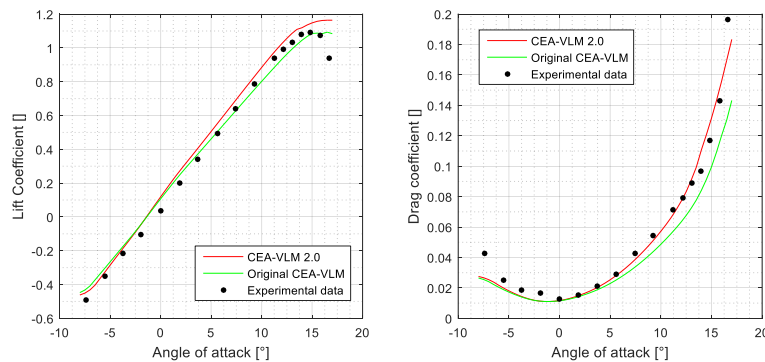


Figure 9. Results comparison for Wing 2

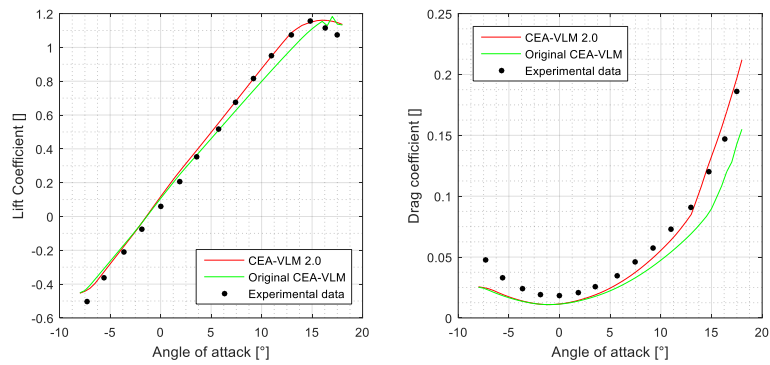


Figure 10. Results comparison for Wing 3

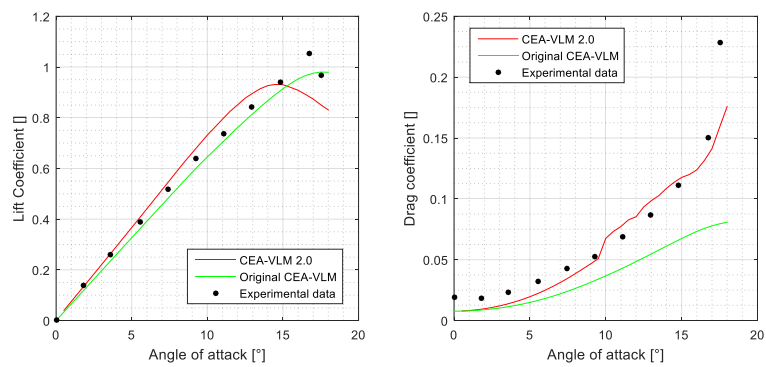


Figure 11. Results comparison for Wing 4

The results in Fig. (11) show that the new implemented method gained a tendency to underestimate the maximum lift coefficient and the stall angle of highly swept surfaces and, in the work of Araújo (2016), it was observed the same behavior for surfaces subjected to a yaw angle. As explained by the author, this happens because of the appearance of a transversal velocity component (in other words, in the span direction) in analyzes of those types, that changes the nature of the boundary layer next to the surface. Since the airfoil data does not consider this type of situation, this creates another error source that is proportional to the transversal velocity value. In an extreme case, this may induce the appearance of convoluted streamlines in the middle of the surface (like the tip vortices), that increases the lift and delays the stall (Anderson, 1984). This limitation is a characteristic of the Lifting Line Method, as explained in Section 2.1.2.

It must be noticed as well that the resulting distribution of lift coefficient and effective angle of attack became more reasonable with the new method, as shown in Fig. (12) and Fig. (13), for the analysis of the Wing 1.

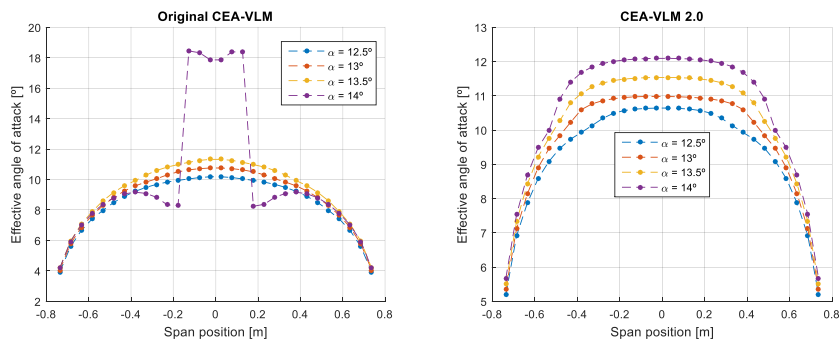


Figure 12. Results for the distribution of the effective angle of attack in the analysis of the Wing 1

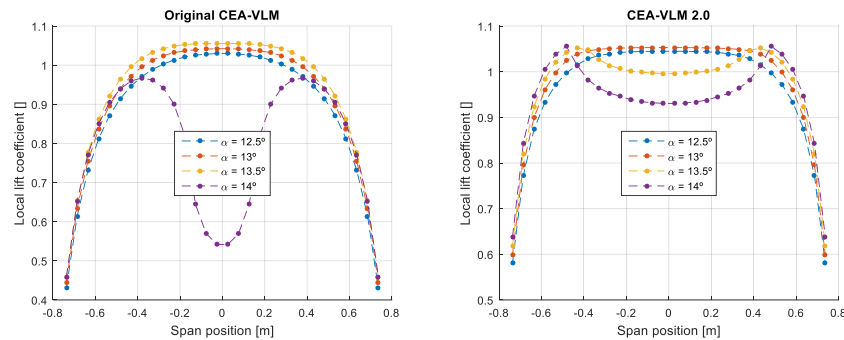


Figure 13. Results for the distribution of the airfoil lift coefficient in the analysis of the Wing 1

5. CONCLUSION REMARKS

The new iterative method implemented in the CEA-VLM code were capable to maintain the convergence even in the analysis subject to the stall of the surfaces. In the tests performed, the distributions of forces, circulation and effective angle of attack were more reasonable.

Comparing the global coefficients with the experimental data, the new code improved the accuracy of the estimation of both the maximum lift coefficient and stall angle. For the linear part of the lift curve, the two methods provide very close results. However, after the stall angle, even with the convergence of the method, in the surfaces analyzed, there was an overestimation of the lift, leading to a “softening” of the stall region.

As mentioned before, since the new method implemented is closer to the Lifting Line Method than the original one, it carries most of its characteristics and limitations, as shown in Section 4. But above all that, with the new iterative method, the software CEA-VLM 2.0 was capable of obtaining better estimates of maximum lift coefficient and stall angle than the original code. However, it must be observed the limitations of the code, bounded to the type of analysis of the flow, truncation errors of the iterative method and the reliability of the airfoil section data.

6. REFERENCES

- Anderson, J.D., 1984. *Fundamentals of Aerodynamics*. McGraw-Hill Book Company, 2nd edition.
- Araújo, A.M., 2016. *Implementação de um algoritmo para melhora da convergência do método vortex-lattice não linear e aprimoramento das estratégias de cálculo de esteira livre no programa CEA-VLM*. Graduation thesis, Federal University of Minas Gerais, Belo Horizonte.
- Chattot, J.-J., 2004. “Analysis and Design of Wings and Wing/Winglet Combinations at Low-Speeds”. In *Computational Fluid Dynamics Journal*, Vol 13(3), p. 76.
- Katz, J., Plotkin, A., 2011. *Low-Speed Aerodynamics*. Cambridge University Press, Cambridge, 2nd edition.
- Mukherjee, R., Gopalarathnam, A., Kim, S.W., 2003. “An iterative decambering approach for post-stall prediction of wing characteristics using known section data”. In *41st AIAA Aerospace Sciences Meeting*. Reno, United States.
- Purser, P.E., Spearman, M.L., 1951. *NACA TN 2445: Wind-tunnel tests at low speed of swept and yawed wings having various plan forms*. Langley Aeronautical Laboratory, Langley.
- Sheldahl, R.E., Klimas, P.C., 1981. *Aerodynamic characteristics of seven symmetrical airfoil sections through 180-degree angle of attack for use in aerodynamic analysis of vertical axis wind turbines*. Sandia National Laboratories, Albuquerque.
- Vargas, L.A.T.D., 2006. *Desenvolvimento e Implementação de um Procedimento Numérico para Cálculo de Conjuntos Asa-Empenagens de Geometria Complexa em Regime de Voo Subsônico*. Master’s Degree thesis, Federal University of Minas Gerais, Belo Horizonte.

7. RESPONSIBILITY NOTICE

The authors are the only responsible for the printed material included in this paper.